Indian Journal of Chemical Technology
Vol. 28, November 2021, pp. 693-700

Optical characterization of different oxide nanomaterials dispersed PVA/PEO blend matrix-based hybrid polymer nanocomposites for advances in optoelectronic device technologies

Priyanka Dhatarwal[1], Shobhna Choudhary*[,2] & R J Sengwa[1]

[1]Dielectric Research Laboratory, Department of Physics, Jai Narain Vyas University, Jodhpur 342 005, India

[2]CSIR-Human Resource Development Centre, Ghaziabad 201 002, India

E-mail: shobhnachoudhary@rediffmail.com

Received 29 June 2021; accepted 30 July 2021

Optical properties of different oxide nanomaterials (viz. zinc oxide (ZnO), tin oxide (SnO_2), silica (SiO_2), and alumina (Al_2O_3)) as nanofillers (NFs) and a host polymer matrix of poly(vinyl alcohol) (PVA)/poly(ethylene oxide) (PEO) blend based hybrid polymer nanocomposites (HPNCs) have been investigated by employing ultraviolet-visible (UV-Vis) spectroscopy. The UV-Vis absorbance spectra over the photons wavelength range 200-800 nm, and the absorption coefficient, energy bandgap, and Urbach energy of the PVA/PEO/NFs HPNC films are determined and reported. The dependence of the optical characteristics of these HPNCs on the type of oxide nanofillers and their concentration have been studied which is found correlated with the optical properties of the nanofillers. Considering the results, suitability of PVA/PEO/NFs materials as potential candidates for UV-shielder, light diffuser, bandgap tuner, and photo-sensor/detector in the design and evolution of various flexible-type optoelectronic devices/components have been discussed.

Keywords: Optical properties, Optoelectronic applications, Oxide nanofillers, Polymer nanocomposites, PVA/PEO blend

In the last decade, several flexible and stretchable-type organic polymer matrices and inorganic nanomaterials based hybrid polymer nanocomposites (HPNCs) were prepared with state-of-the-art and characterized to confirm their uses as multifunctional promising materials in advances of polymer engineering and technology based lightweight, cost-effective, and miniaturized electronic devices[1–11]. Most of the HPNCs were characterized for confirmation of their appropriately controllable morphological, nanostructural, thermal, mechanical, dielectric, electrical, and optical properties in order to meet tremendously increased industrial demand[2–5,9–12].

Due to good water solubility, biodegradability, hydrophilic character, and flexible film-forming ability of the polar PVA/PEO blend material, its matrix is widely considered in producing a variety of technological useful flexible-type nanocomposite materials for next-generation devices/components[8,13–16]. The PVA/PEO blend matrix is preferred for the preparation of several promising solid polymer electrolytes (SPEs) for the energy-storing devices[16–18], and also fabricating novel HPNCs for various applications including the potential candidates in the fabrication of biodegradable-type microelectronic and optoelectronic devices[13–15,19–25].

In the past few years, the authors have developed the PVA/PEO/SnO_2 films[26], PVA/PEO/ZnO films[27], PVA/PEO/SiO_2 films[28], and PVA/PEO/Al_2O_3 films[29] by solution-cast method and investigated their structural, dielectric, and electrical properties for confirmation of suitability as flexible-type biodegradable nanodielectrics for advances in microelectronic technologies. The nanofillers used in the preparation of these HPNCs are of different structural properties i.e., the SiO_2 is amorphous[7,28], Al_2O_3 has γ-phase[29], ZnO has hexagonal wurtzite[4], and SnO_2 has tetragonal rutile[26] crystal which also influence the various properties of the HPNC materials. It has been noted that the dielectric and electric properties of these PNCs can be practically tuned by varying the filler concentration and altering the type of oxide nanofiller. Furthermore, the SnO_2 and ZnO nanomaterials belong to wide energy bandgap metal oxide semiconductors[4,9,12,30] which are highly important from an optoelectronic device materials point of view to adjust the bandgap in a wide range and also the absorption of photons energy in the

HPNC materials containing these nanofillers[4,7,9,11,12]. In contrast to SnO_2 and ZnO materials, the SiO_2 and Al_2O_3 nanomaterials are of extremely high optical energy bandgap[31,32] and are frequently dispersed in the polymer matrix to set the bandgap of the composite in a narrow range and also to improve their thermo-mechanical properties[9,33,34].

A survey of the literature reveals that there is a lack of systematic optical characterization of the PVA/PEO/ZnO, PVA/PEO/SnO_2, PVA/PEO/SiO_2, and PVA/PEO/Al_2O_3 HPNC films which are needed for confirmation of their suitability in biodegradable optoelectronics, and therefore in this manuscript these HPNCs are studied using UV-Vis spectroscopy and their detailed optical properties are presented.

Experimental Section

Materials

The PVA (M_w = 77×10^3 g mol^{-1}) of the Loba Chemie, India, and PEO (M_w = 6×10^5 g mol^{-1}) of Sigma-Aldrich, USA and the nanopowders of various inorganic oxides having different particle sizes t_p of Sigma-Aldrich Co., i.e., ZnO (t_p< 100 nm; SKU 544906, a product of USA), SnO_2 (t_p≤ 100 nm; SKU 549657, a product of USA), SiO_2 (5≤ t_p≤15 nm; SKU 637246, a product of USA), and Al_2O_3 (t_p≤ 50 nm; SKU 544833, a product of Austria) are taken for the preparation of various HPNC films.

PVA/PEO/NFs films containing the PVA/PEO blend matrix of 50/50 wt% dispersed with x wt% amounts of NFs (x = 0, 1, 3, and 5 wt% in comparison to the weight of polymer blend) were prepared by the aqueous solution-casting method. The details of various steps followed for the preparation of these different oxide nanofillers loaded HPNC films and their successful nanocomposite formation are demonstrated in the recent publications[26–29].

Measurements

The UV-Vis absorbance spectra over the wavelength range 200–800 nm for these PVA/PEO/NFs HPNC films were recorded at ambient temperature by a dual-beam UV-Vis spectrophotometer of Agilent Technologies (Model: Cary 60) which is equipped with a solid sample holder and fully controlled by the Cary Win UV Scan application software. For the measurements, each film of thickness t was mounted in the solid sample holder keeping the film surface exactly normal to the direction of incident photons. The measurements of absorbance spectra of these HPNC films were performed with the baseline correction at a wavelength accuracy of 1 nm and keeping the scan speed of 600 nm/min.

Results and Discussion

Analysis of absorbance spectra

The UV-Vis absorbance spectra of PVA/PEO/NFs films with varying nanofillers concentrations (0–5 wt%) are provided in Fig. 1a-d. This figure clearly revealed that the PVA/PEO film has significant absorbance (A) over the entire visible region (800–400 nm) which further increased in the UV-region of 400 to 280 nm (i.e., for UV-A, UV-B and partially UV-C radiations) and lastly exhibited strong absorption band having an onset wavelength of about 250 nm. The higher absorption for the visible range photons by the PVA/PEO film is related to partially opaque character of the PEO material[35] and the high optical transparency of PVA film[36]. The revealed absorbance band with a maximum at about 200 nm evidences the n–π^* electronic transitions in the PVA/PEO blend material for the higher energy UV photons[24].

It is examined from Fig. 1 that in comparison to the PVA/PEO film, the absorbance is higher for all the different oxide NFs (ZnO, SnO_2, SiO_2, and Al_2O_3) loaded PVA/PEO/NFs films which enhanced systematically with the increase of filler concentration and largely varied with the type of nanomaterial loaded in the PVA/PEO blend matrix. Additionally, the absorbance band onset wavelength exhibited a redshift with the increase of nanofiller concentration in these HPNC materials. These UV-Vis absorbance characteristics corroborate with a variety of HPNC materials studied previously[4,5,9,11,19,24,33–36]. The increase in absorbance with the increase of NFs contents in the PVA/PEO/NFs composites is definitely due to some scattering of photons and increase in the opaque character of the films, whereas the redshift of the absorption band is a sign of charge transfer complexes (CTCs) developed in these HPNC films explained for several other HPNC materials[9,17,24,33,36]. Among these different nanomaterials containing HPNCs, the absorbance is found relatively high for the SnO_2 nanoparticles loaded HPNC films (see Fig. 1b) which saturate in the UV-region at 5 wt% concentration suggesting the suitability of this PVA/PVP/5 wt% SnO_2 nanocomposite system as an excellent UV blocker/shielder similar to some other materials[5,9,37]. It is also noted that the ZnO nanoparticles loaded HPNCs exhibited a surface plasmon resonance (SPR) peak of

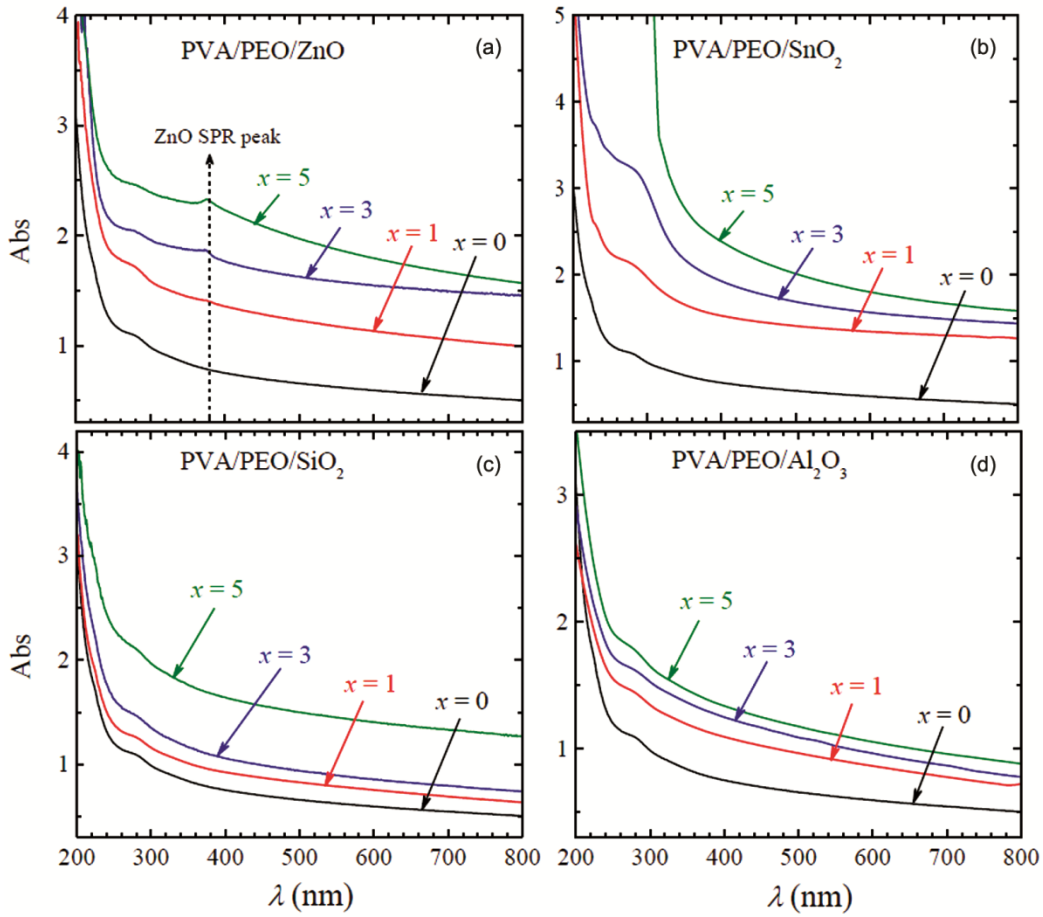

Fig. 1 — Plots of absorbance (Abs) versus wavelength (λ) for PVA/PEO/NFs HPNC films with varying concentration *x* (wt%) of the nanofillers (NFs); **(a)** PVA/PEO/*x* wt% ZnO, **(b)** PVA/PEO/*x* wt% SnO_2, **(c)** PVA/PEO/*x* wt% SiO_2, and **(d)** PVA/PEO/*x* wt% Al_2O_3.

the ZnO NPs at 375 nm which is marked in Fig. 1a and its presence corroborated with most of the HPNC materials prepared with ZnO loading and studied earlier[4,9,36–38]. Furthermore, Fig. 1c and d explain that the absorbance is relatively low for the SiO_2 and Al_2O_3 loaded PVA/PEO/NFs films but it is reasonably controllable with the concentration of the NFs. From these findings, it is suggested that these HPNC materials can be potential candidates to be used as light diffuser coating which is needed for packaging of numerous optoelectronic devices/components[3–5,9,12,37,38].

Wavelength dependent absorption coefficient

The study of incident photons wavelength (λ) dependent absorption coefficient (α) of the HPNC materials is highly meaningful owing to its involvement in the Tauc's plots for the determination of their energy band gaps (direct and indirect) and Urbach energy related to the electronic transitions[9,34,37]. The α value represents the amount of incident photon intensity absorbed per unit thickness by an optical material under test acting as a light absorber. It is directly related to the absorbance parameter *A* by Beer-Lambert law A as $\alpha = 2.303\ A/t$, where *t* is the thickness of the material and *A* is dependent on the intensity of photon input (I_0) and output (I) given by the relation $A = \log (I_0/I)$.

Fig. 2 shows the α versus λ plots for the PVA/PEO/NFs films containing different oxides NFs (SnO_2, ZnO, SiO_2, and Al_2O_3). It can be understood from this figure that the λ dependent α values of the investigated composite films in principle obey the shape of absorbance spectra (given in Fig. 1) with the variation of photons wavelength as well as the increase in the concentration of NFs in the PVA/PEO blend host matrix. It is expected because the α is directly related to the absorbance of the material.

Energy bandgap

The optical energy band gap E_g of the HPNC materials is one of the most significant parameters for deciding their optoelectronic applications[4,5,9–14,19,24,33–38].

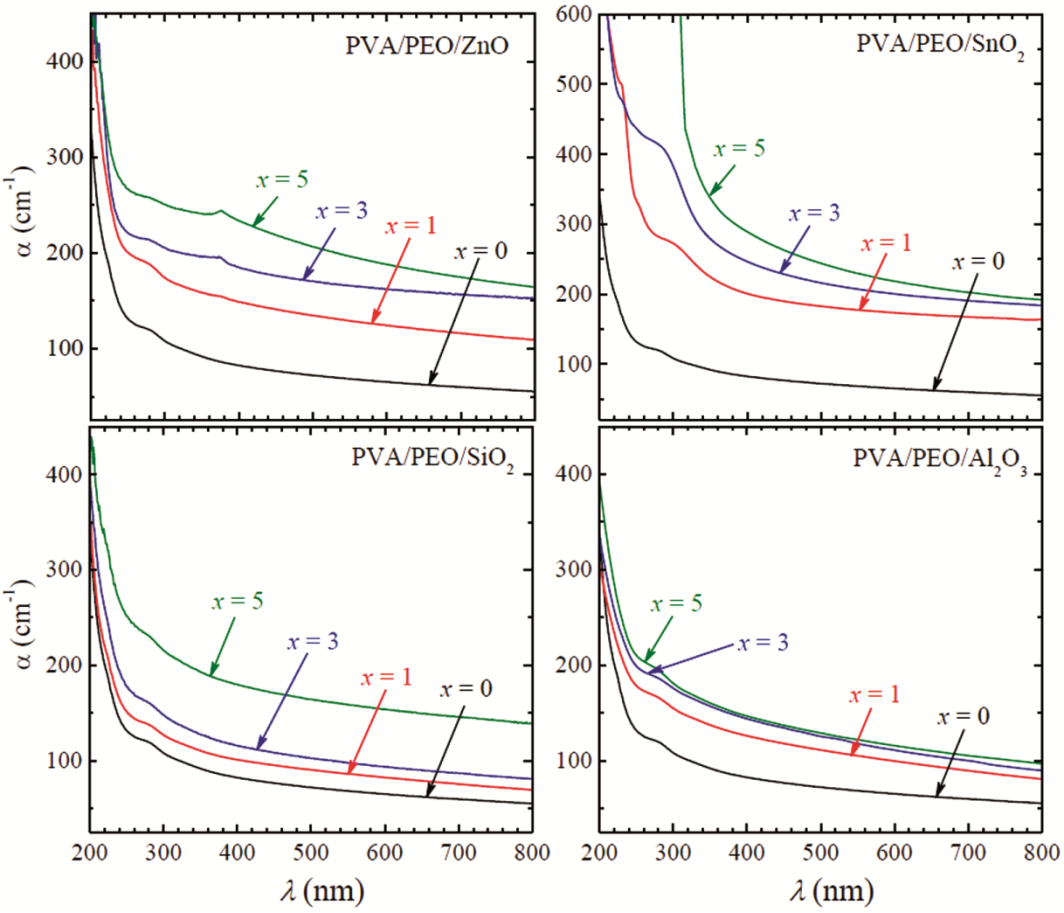

Fig. 2 — Plots of absorbance coefficient (α) versus wavelength (λ) for PVA/PEO/NFs HPNC films with varying concentration *x* (wt%) of the nanofillers (NFs); **(a)** PVA/PEO/*x* wt% ZnO, **(b)** PVA/PEO/*x* wt% SnO_2, **(c)** PVA/PEO/*x* wt% SiO_2, and **(d)** PVA/PEO/*x* wt% Al_2O_3.

Various type of E_g values of an optical material are in principle computed by applying Davis and Mott relation[39] $(\alpha h\nu)^m = B(h\nu - E_g)$ and this relation-based Tauc's plots[40] ($(\alpha h\nu)^m$ versus $h\nu$) for different m values. In this relation, $h\nu$ is the photon energy at a frequency of ν, h is Plank constant, B is constant of proportionality, and the m is variable which is set 1 and ½ values for determination of direct bandgap E_{gd} and indirect bandgap E_{gi}, respectively. The wavelength λ (nm) dependent $h\nu$ (eV) values could be computed by the simple relation $h\nu = 1240/\lambda$.

Fig. 3 depicts the Tauc's plots ($(\alpha h\nu)^2$ versus $h\nu$) for these different oxides NFs containing PVA/PEO/NFs films for the determination of their E_{gd} values. The E_{gd} values of these materials were obtained by extrapolation procedure demonstrated in detail previously[33,37]. The E_{gd} values of various HPNC films noted from their Tauc's plots at different concentrations of nanofillers *x* (wt%) are listed in Table 1 and additionally plotted as a function of nanofiller concentration *x* (wt%) in the insets of this figure for the benefit of readers. From the table and these insets, it can be noted that for all these NFs containing HPNCs, the E_{gd} values decrease with the increase of nanofiller concentration but the decrease depends on the type of NF and its optical bandgap. The E_g value of SnO_2 (E_g = 3.6 eV)[30] and ZnO (E_g = 3.3 eV)[4,36–38] are much lower than that of the PVA/PEO blend matrix bandgap (E_g = 5.6 eV) obtained in this work. Therefore, the decrease in E_{gd} values of PVA/PEO/ZnO and PVA/PEO/SnO_2 with increase in their amount are expected with the loading of ZnO and SnO_2 in the PVA/PEO blend matrix. Additionally, it is found that the decrease is very high for the SnO_2 loaded HPNCs in which the bandgap of 3 wt% and 5 wt% SnO_2 containing films are found close to that of the pure SnO_2 material. Such decrease in E_{gd} values with the increase of SnO_2 amount in the host polymer matrix is also reported in the literature for several other polymer matrices based SnO_2 loaded HPNC materials[9,12,37].

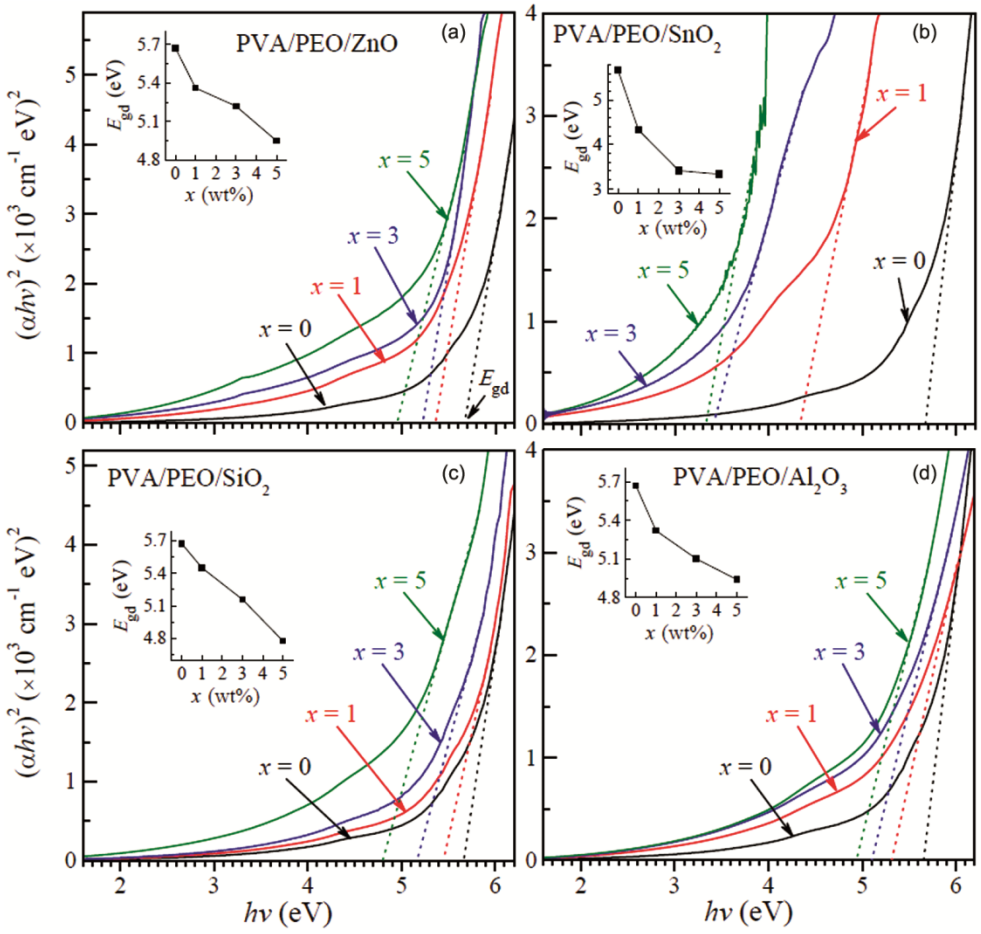

Fig. 3 — Tauc's plots ($(\alpha h\nu)^2$ versus $h\nu$) for PVA/PEO/NFs HPNC films with varying concentration x (wt%) of the nanofillers (NFs); **(a)** PVA/PEO/x wt% ZnO, **(b)** PVA/PEO/x wt% SnO_2, **(c)** PVA/PEO/x wt% SiO_2, and **(d)** PVA/PEO/x wt% Al_2O_3.

Table 1 — The values of direct energy bandgap E_{gd}, indirect energy bandgap E_{gi}, and Urbach energy E_u of the PVA/PEO/NFs HPNC films.

HPNC films x (wt%)	E_{gd} (eV)	E_{gi} (eV)	E_u (eV)
PVA/PEO/x wt% ZnO films			
0	5.67	4.39	1.38
1	5.36	4.08	1.68
3	5.22	3.92	1.94
5	4.95	3.42	2.36
PVA/PEO/x wt% SnO_2 films			
1	4.33	3.71	2.08
3	3.41	-	2.32
5	3.33	-	2.66
PVA/PEO/x wt% SiO_2 films			
1	5.45	4.09	1.74
3	5.16	3.32	2.11
5	4.78	2.64	2.99
PVA/PEO/x wt% Al_2O_3 films			
1	5.32	3.06	2.89
3	5.10	2.84	3.21
5	4.94	2.76	3.40

The decrease in E_{gd} values of PVA/PEO/SiO_2 and PVA/PEO/Al_2O_3 films is also noted with the increase of SiO_2 and Al_2O_3 concentrations although the SiO_2 material bandgap is E_g = 5.5 eV[31] which is close to that of the PVA/PEO blend matrix but Al_2O_3 material has significantly high bandgap (E_g = 7.6 eV)[32]. The decreasing E_{gd} values of SiO_2 and Al_2O_3 containing these HPNCs infer that there is the formation of localized states within the forbidden energy band gap of the PVA/PEO material which supports the electronic transition from the valence band to the conduction band and hence the bandgap of such types of composites decrease[33,34,37,41,42].

The indirect bandgap E_{gi} values of these PVA/PEO/NFs materials were also determined from their $(\alpha h\nu)^{1/2}$ versus $h\nu$ Tauc's plots given in Fig. 4. The E_{gi} values estimated for these HPNC materials are listed in Table 1. One can examine from this table that the E_{gi} values of PVA/PEO/NFs significantly changed with the type of filler and its concentration.

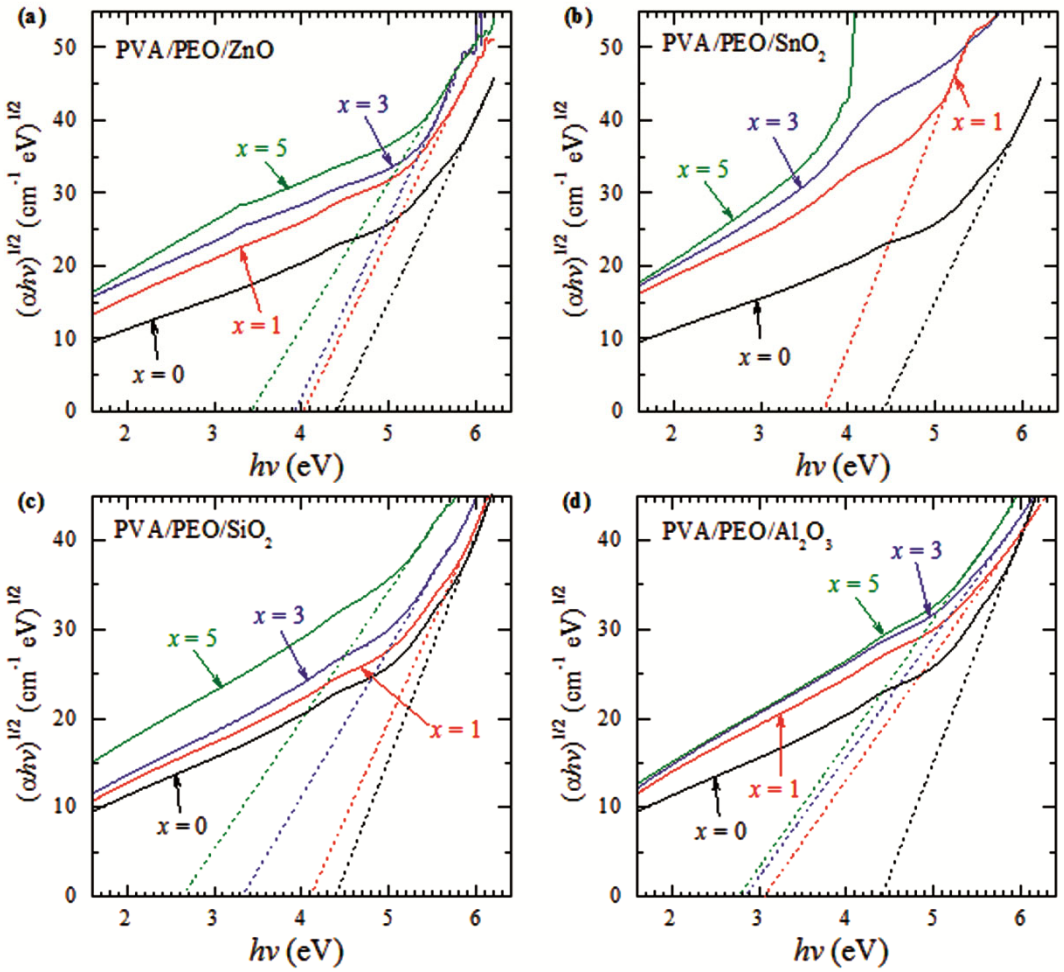

Fig. 4 — Tauc's plots ($(\alpha h\nu)^{1/2}$ versus $h\nu$) for PVA/PEO/NFs HPNC films with varying concentration x (wt%) of the nanofillers (NFs); **(a)** PVA/PEO/x wt% ZnO, **(b)** PVA/PEO/x wt% SnO_2, **(c)** PVA/PEO/x wt% SiO_2, and **(d)** PVA/PEO/x wt% Al_2O_3.

Further, it is found that the E_{gi} values are lower than that of the respective E_{gd} values for these HPNC materials which are in agreement with the behaviour of E_{gi} and E_{gd} values reported previously for other HPNC materials[12,33,34,37].

Urbach energy and behaviour of electronic transitions

Urbach energy E_u of the HPNC materials ~~are~~ is frequently determined to confirm the tail width of localized states arising in the forbidden energy bandgap as a consequence of structural disordering. These tail states formed in the forbidden energy bandgap exists either right above the valence band or just below the start of the conduction band in a hybrid material. The band tail states originate from several structural disorder sources like alteration by hetero-interaction, thermal variation, impurity mixing or absorbed from the environment, and compositional constituents variation but its behaviour obeys the exponential distribution given by relation $\alpha = \alpha_0 \exp(h\nu/E_u)$[36,37,42], where α_0 is a pre-exponent factor. If the plot is linear between the $ln\alpha$ versus $h\nu$ around the fundamental absorption edge then the slope value of this linear plot is numerically equal to the reciprocal of the E_u value. Fig. 5 demonstrates that all the PVA/PEO/NFs materials have the linear behaviour of their $ln\alpha$ versus $h\nu$ plots near absorption edge and therefore the E_u values were computed from these linear plots and recorded in Table 1. The E_u values of these HPNCs showed an increasing trend with the increase of filler concentration which evidences the creation of a large number of structural defects ~~g~~ in the forbidden energy band gap of the PVA/PEO blends which favours the decrease in their bandgap values. Furthermore, from Table 1, it can be noted that the E_u values also depend on the type of nanofillers and their concentration in the PVA/PEO/NFs materials.

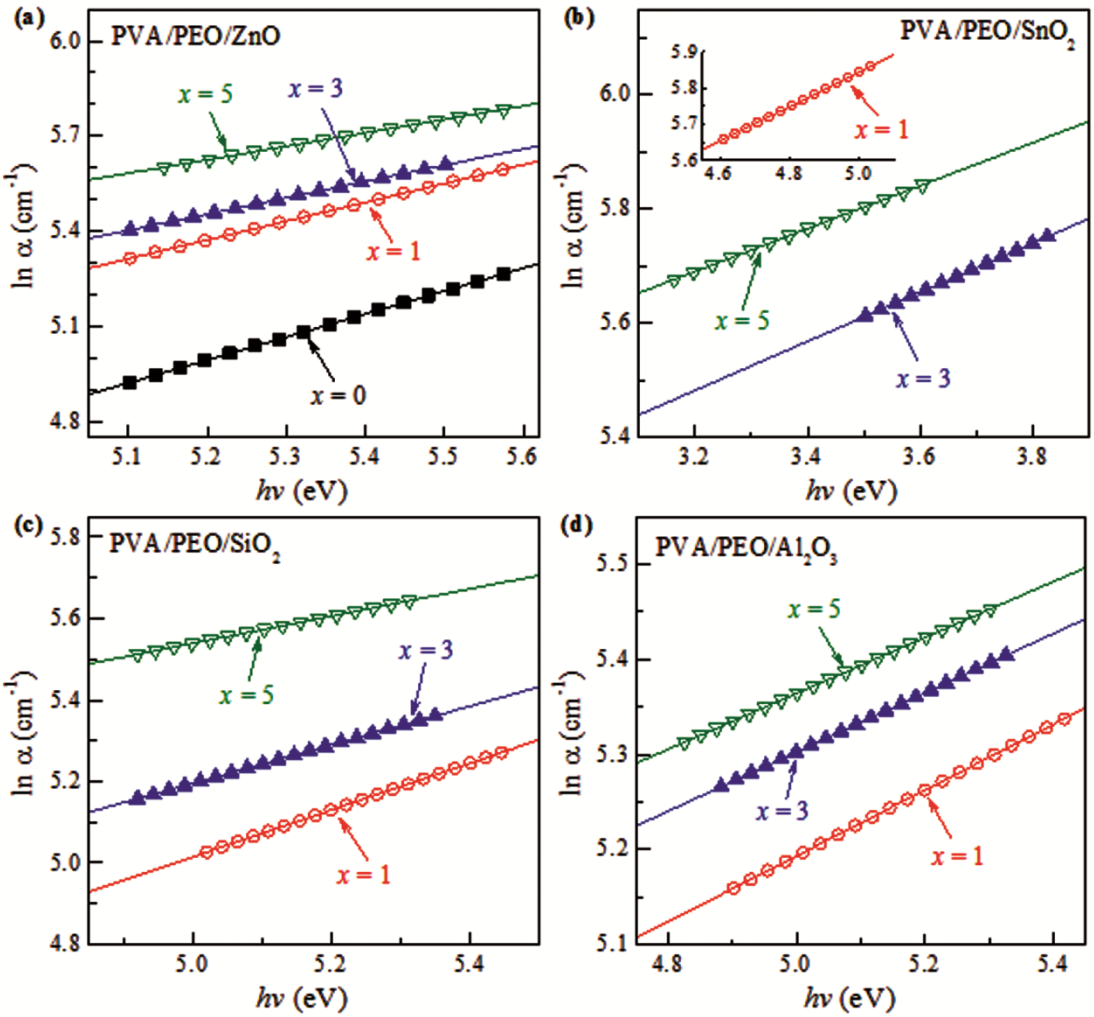

Fig. 5 — Plots of logarithmic absorption coefficient ($ln\alpha$) versus $h\nu$ for PVA/PEO/NFs HPNC films with varying concentration x (wt%) of the nanofillers (NFs); **(a)** PVA/PEO/x wt% ZnO, **(b)** PVA/PEO/x wt% SnO_2, **(c)** PVA/PEO/x wt% SiO_2, and **(d)** PVA/PEO/x wt% Al_2O_3.

Conclusion

This manuscript provides the detailed optical properties of the PVA/PEO/NFs HPNC films of different NFs (ZnO, SnO_2, SiO_2, and Al_2O_3) with their concentration varying from 0 to 5 wt%. All these HPNC materials have increased absorbance and decreased bandgap with the increase of NF concentrations. The ZnO, SiO_2, and Al_2O_3 nanofillers loading provided a narrow range bandgap adjustment with their loadings up to 5 wt% in the PVP/PEO blend matrix, whereas SnO_2 concentration altered the bandgap in a wider range. The absorbance and energy bandgap behaviour with changing the oxide nanomaterials and their concentration confirm the suitability of these HPNCs in the development of next-generation flexible-type optoelectronic devices like sensors, detectors, filters, and also as potential candidates for light diffusers and UV shielders.

Acknowledgements

One of the authors (PD) thanks the CSIR, New Delhi for the award of a postdoctoral research associate fellowship.

References

1 Pielichowski K & Majka T, Polymer Composites with Functionalized Nanoparticles, Elsevier Inc., (Amsterdam), (2019).

2 Guo J G, Song K & Liu C, Polymer-based Multifunctional Nanocomposites and their Applications. Elsevier Inc., (Amsterdam), (2019).

3 Ponnamma D, Sadasivuni K K, Cabibihan J J & Al-Maadeed M A A, Smart Polymer Nanocomposites: Energy Harvesting, Self-Healing and Shape Memory Applications. Springer International Publishing, (Switzerland), (2017).

4 Sengwa R J & Choudhary S, *Curr Appl Phys*, 18 (2018) 1041.
5 Sengwa R J, Choudhary S & Dhatarwal P, *J Mater Sci Mater Electron*, 30 (2019) 12275.
6 Tan D Q, *Adv Func Mater*, 30 (2020) 1808567.
7 Sengwa R J, Dhatarwal P & Choudhary S, *Mater Today Commun*, 25 (2020) 101380.
8 Sengwa R J, Choudhary S & Sankhla S, *Comps Sci Technol*, 70 (2010) 1621.
9 Sengwa R J & Dhatarwal P, *Optical Mater*, 113 (2021) 110837.
10 Dhatarwal P & Sengwa R J, *Funct Compos Struct*, 3 (2021) 025008.
11 Dhatarwal P, Sengwa R J & Choudhary S, *Optik*, 221 (2020) 165368.
12 Sengwa R J & Dhatarwal P, *J Mater Sci Mater Electron*, 32 (2021) 9661.
13 Elashmawi I S, Abdelrazek E M, Hezma A M & Rajeh A, *Physica B*, 434 (2014) 57.
14 Ragab H M, *Results Phys*, 7 (2017) 2057.
15 Tang J, Liu X, Ge Y & Wang F, *Molecules*, 26 (2021) 2783.
16 Putri R M, Sundari C D D, Floweri O, Mayangsari T R, Ivansyah A L, Santosa S P, Arcana M & Iskandar F, *J Non-Cryst Solids*, 556 (2021) 120549.
17 Aziz S B, Abdullah O Gh, Hussein A M, Abdulwahid R T, Rasheed M A, Ahmed H M, Abdalqadir S W & Mohammed A R, *J Mater Sci Mater Electron*, 28 (2017) 7473.
18 Xu L, Wei K, Cao Y, Ma S, Li J, Zhao Y, Cui Y & Y Cui, *RSC Adv*, 10 (2020) 5462.
19 Farea M O, Abdelghany A M, Meikhail M S & Oraby A H, *J Mater Res Technol*, 9 (2020) 1530.
20 He M, Chen M, Dou Y, Ding J, Yue H, Yin G, Chen X & Cui Y, *Polymers*, 12 (2020) 305.
21 Hadi A, Hashim A & Al-Khafaji Y, *Trans Electr Electron Mater*, 21 (2020) 283.
22 Hashim A, Al-Khafaji Y & Hadi A, *Trans Electr Electron Mater*, 20 (2019) 530.
23 Jebur Q M, Hashim A & Habeeb M A, *Trans Elect Electron Mater*, 20 (2019) 334.
24 Abd El-Kader M F H & Elabbasy M T, *J Mater Res Technol*, 9 (2020) 16179.
25 Abd El-kader F H, Hakeem N A, Elashmawi I S & Ismail A M, *Indian J Phys*, 87 (2013) 983.
26 Choudhary S, Dhatarwal P & Sengwa R J, *Indian J Chem Technol*, 27 (2020) 367.
27 Choudhary S, *Physica B*, 522 (2017) 48.
28 Choudhary S, *Indian J Eng Mater Sci*, 23 (2016) 399.
29 Choudhary S, *Indian J Chem Technol*, 25 (2018) 51.
30 Orlandi M O, Tin Oxide Materials: Synthesis, Properties, and Applications, Elsevier Inc. (Amsterdam) (2020).
31 Tański T, Matysiak W, Krzemiński Ł, Jarka P & Gołombek K, *Appl Surf Sci*, 424 (2017) 184.
32 Filatova E O & Konashuk A S, *J Phys Chem C*, 119 (2015) 20755.
33 Dhatarwal P & Sengwa R J*, Physica B*, 613 (2021) 412989.
34 Dhatarwal P & Sengwa R J, *Optik*, 233 (2021) 166594.
35 Morsi M A, Rajeh A & Al-Muntaser A A, *Compos Part B*, 173 (2019) 106957.
36 Soliman T S, Rashad A M, Ali I A, Khater S I & Elkalashy S I, *Phys Status Solidi*, 217 (2020) 2000321.
37 Dhatarwal P & Sengwa R J, *Optik*, 241 (2021) 167215.
38 Dhatarwal P & Sengwa R J, *Compos Interfaces*, 28 (2021) 827.
39 Davis E A & Mott N F, *Philos Mag*, 22 (1970) 903.
40 Tauc J, Optical Properties and Electronic Structure of Amorphous Semiconductors. In: Nudelman S, Mitra S S (eds) Optical Properties of Solids. Optical Physics and Engineering. Springer, (Boston), (1969).
41 Dhatarwal P, Choudhary S & Sengwa R J, *J Polym Res*, 28 (2021) 63.
42 Soliman T S, Vshivkov S A & Elkalashy S I, *Polym Compos*, 41 (2020) 3340.